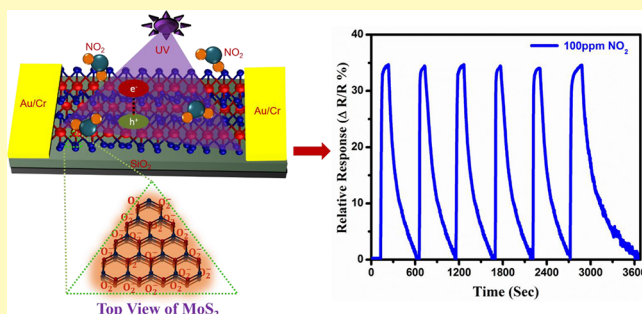


UV-Activated MoS₂ Based Fast and Reversible NO₂ Sensor at Room Temperature

 Rahul Kumar,[†] Neeraj Goel,[†] and Mahesh Kumar*,[†]
[†]Department of Electrical Engineering, Indian Institute of Technology Jodhpur, Jodhpur-342011, India

S Supporting Information

ABSTRACT: Two-dimensional materials have gained considerable attention in chemical sensing owing to their naturally high surface-to-volume ratio. However, the poor response time and incomplete recovery at room temperature restrict their application in high-performance practical gas sensors. Herein, we demonstrate ultrafast detection and reversible MoS₂ gas sensor at room temperature. The sensor's performance is investigated to NO₂ at room temperature, under thermal and photo energy. Incomplete recovery and high response time of ~249 s of sensor are observed at room temperature. Thermal energy is enough to complete recovery, but it is at the expense of sensitivity. Further, under photo excitation, MoS₂ exhibits an enhancement in sensitivity with ultrafast response time of ~29 s and excellent recovery to NO₂ (100 ppm) at room temperature. This significant improvement in sensitivity (~30%) and response time (~88%) is attributed to the charge perturbation on the surface of the sensing layer in the context of NO₂/MoS₂ interaction under optical illumination. Moreover, the sensor shows reliable selectivity toward NO₂ against various other gases. These unprecedented results reveal the potential of 2D MoS₂ to develop a low power portable gas sensor.



KEYWORDS: 2D MoS₂, CVD, gas sensor, NO₂, photo excitation, selectivity

The emission of toxic gases from industrial processes, automotive engines, nuclear test, and power plants is intrinsic to increasing environmental pollution, which affects the health of living species severely.¹ Therefore, ultrafast detection of hazardous gases in the atmosphere is a stringent necessity for a healthy ambience. For detecting environmental pollutants, two-dimensional (2D) material based sensors have led to a rapid paradigm shift in gas sensing owing to its naturally high surface-to-volume ratio.^{2–5} Among the 2D materials, graphene is one of the most preeminent materials for its excellent conductivity, high mechanical strength, and outstanding electronic and optical properties. These remarkable properties have attracted researchers' interest in electronic device applications such as FET, photodiode, and gas sensor.^{6–8} The graphene based gas sensor has shown sensing of even a single gas molecule (NO₂) at room temperature.⁹

In recent years, transition metal dichalcogenide (TMDCs) materials analogous to graphene are being stimulated in gas sensing applications. MoS₂ being the representative of the TMDCs family modulates its bandgap having a different number of layers. Monolayer MoS₂ has a direct bandgap of ~1.8 eV, while multilayer (>8 L) MoS₂ has an indirect bandgap of ~1.2 eV.¹⁰ The modulation in the bandgap of MoS₂ is attributed to quantum confinement and changing the hybridization in between d orbitals and s orbitals of molybdenum atoms and sulfur atoms, respectively.¹¹ Interestingly, multilayer MoS₂ shows high current flow capability compared to that of

monolayer because of having three times higher density of states.¹² In addition, chemically grown as well as mechanically exfoliated multilayer MoS₂ has been reported for better sensing performance toward NO₂, NH₃, NO, and organic analytes than monolayer MoS₂.¹³ Among several gases, NO₂ is one of the most hazardous gases even at a very low concentration (subppm) and causes serious diseases such as heart failure, asthma, and other respiratory ailments.¹⁴ Therefore, ultrafast detection of NO₂ (subppm concentration) at room temperature in the atmospheric environment is of paramount importance for human health.

Hai-li et al. reported that mechanically exfoliated multilayer MoS₂ showed high sensitivity down to a low 0.8 ppm concentration of NO in comparison to the monolayer (which has unstable current).¹⁵ Recently, Liu et al. showed chemically grown MoS₂ transistor based gas sensor which showed low detection limit of 200 ppb and 1 ppm for NO₂ and NH₃, respectively, at room temperature.¹⁶ These reports were oriented on high sensitivity and low concentration detection, but showed high response time as well as incomplete recovery at room temperature. Besides the high response to low concentration, fast detection and complete recovery are also important for MoS₂ to realize as a reliable and practical gas

Received: October 2, 2017

Accepted: November 1, 2017

Published: November 1, 2017

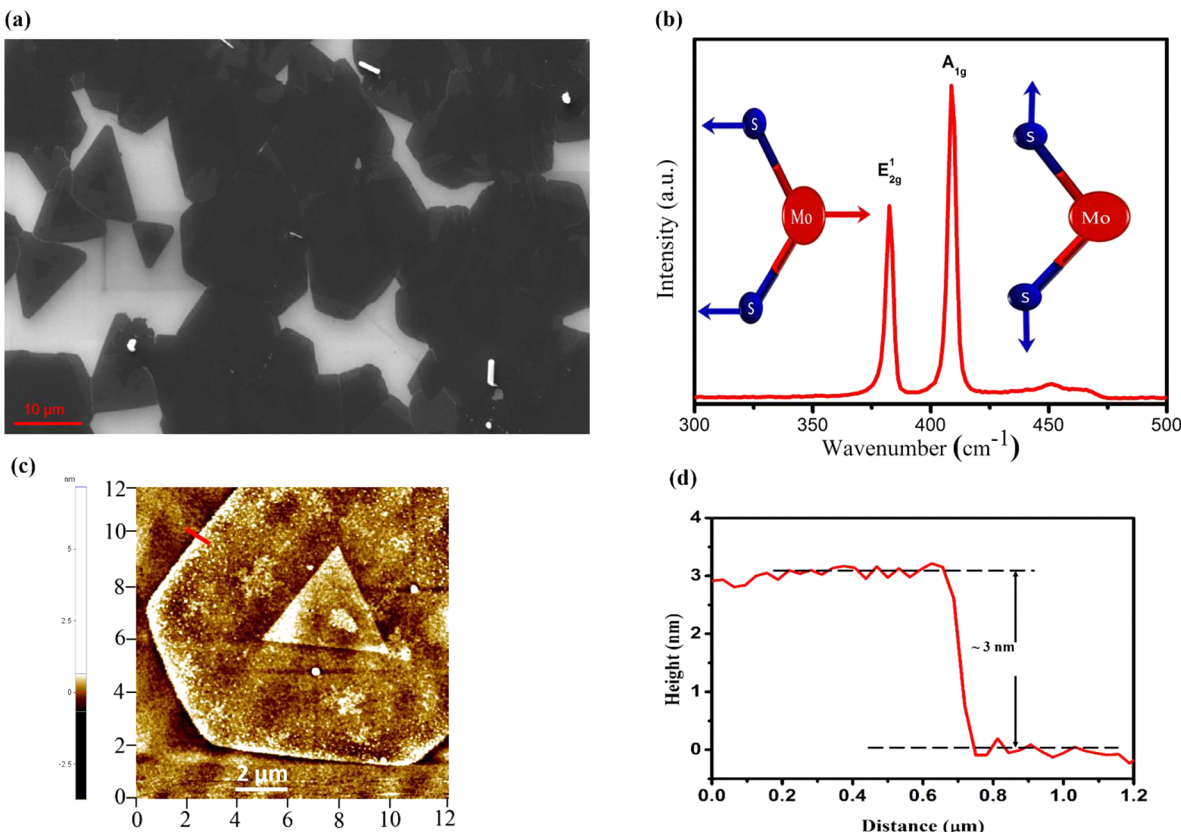


Figure 1. (a) SEM image of triangular shaped combined MoS₂ flakes. (b) Raman spectra of MoS₂. The inset shows the vibration of the Mo (red) and S (blue) atoms related to their two vibrational modes (E_{2g}^1 and A_{1g}). (c) AFM image of MoS₂ flake. (d) Height profile of multilayer MoS₂ flake along the red line in AFM image.

sensor. Poor response time and incomplete recovery to NO₂ of MoS₂ gas sensor prevent its effective use for practical gas sensing applications at room temperature. Cho et al. have reported that recovery of the MoS₂ sensor was improved at the expense of sensitivity by providing thermal energy.¹⁷ This phenomenon was also observed in many recent reports on 2D material based gas sensor.^{18,19} The deterioration in the response of the sensor was attributed to fast desorption of gas molecules (high desorption rate) from sensing layer at high temperature.²⁰ As a result, the increased temperature of the device by thermal energy decreases the sensitivity of 2D materials based gas sensor and also leads to high power consumption. Moreover, adding some extra heating element hampers the portability of the gas sensor. In addition, some efforts have been made in the development of a fast and reversible gas sensor using heterostructure or nanocomposites of MoS₂. For example, Long et al. presented fast detection (response time <1 min) and complete recovery (<1 min) to NO₂ with the expense of sensitivity at 200 °C using MoS₂/graphene hybrid aerogel,¹⁹ and Kuru et al. showed a response time of 40 s and a recovery time of 83 s to H₂ at room temperature using MoS₂ nanosheet–Pd nanoparticle composite.³³ However, nanocomposite or hybrid of MoS₂ approach increases the fabrication steps, complexity, as well as cost of the device. Therefore, another approach is required to achieve full recovery, low cost, without reducing the response of MoS₂ at room temperature. Optical energy has improved the sensing performance of metal oxide, graphene, and CNT sensor at room temperature.^{21–25} Optical energy activates the sensing layer by phonon energy transfer in lieu of thermal energy and

enhances the population of charge carrier as well as reduces the Schottky barrier of the metal contact. Recently, Khan et al. reported enhancement in the current of multilayer MoS₂ in the N₂ gas environment compared to the atmospheric environment under deep UV (220 nm) illumination.²⁶ So, a UV light source can be considered an efficacious technique to improve the sensing performance of the MoS₂ gas sensor at room temperature.

In this article, we fabricated a resistive gas sensor using 2D MoS₂, which was grown by the chemical vapor deposition (CVD) technique on 300 nm SiO₂/Si. The morphology, number of layers, and crystallinity of MoS₂ were investigated by SEM and Raman spectroscopy, respectively. Further, we demonstrate the gas sensing behavior of MoS₂ to subppm concentration NO₂ at room temperature and at 100 °C temperature. In addition, we have also examined the sensing behavior of MoS₂ gas sensor at room temperature under UV illumination. The decrement in response to NO₂ using thermoactivation and enhancement in response as well as ultrafast detection with complete recovery at room temperature of the MoS₂ gas sensor under optical energy are also discussed in detail.

EXPERIMENTAL SECTION

Synthesis of 2D MoS₂. The MoS₂ was controllably grown on 300 nm SiO₂/Si by using conventional CVD process. Prior to growth, the SiO₂ substrate was cleaned by a standard chemical process. The substrate was placed precisely in the face-down position on MoO₃ (0.03 g) powder. Sulfur (1.0 g) was placed in another alumina boat 15 cm away from MoO₃. Horizontally aligned MoS₂ was grown by heating MoO₃ at 870 °C for 60 min and the temperature was raised at

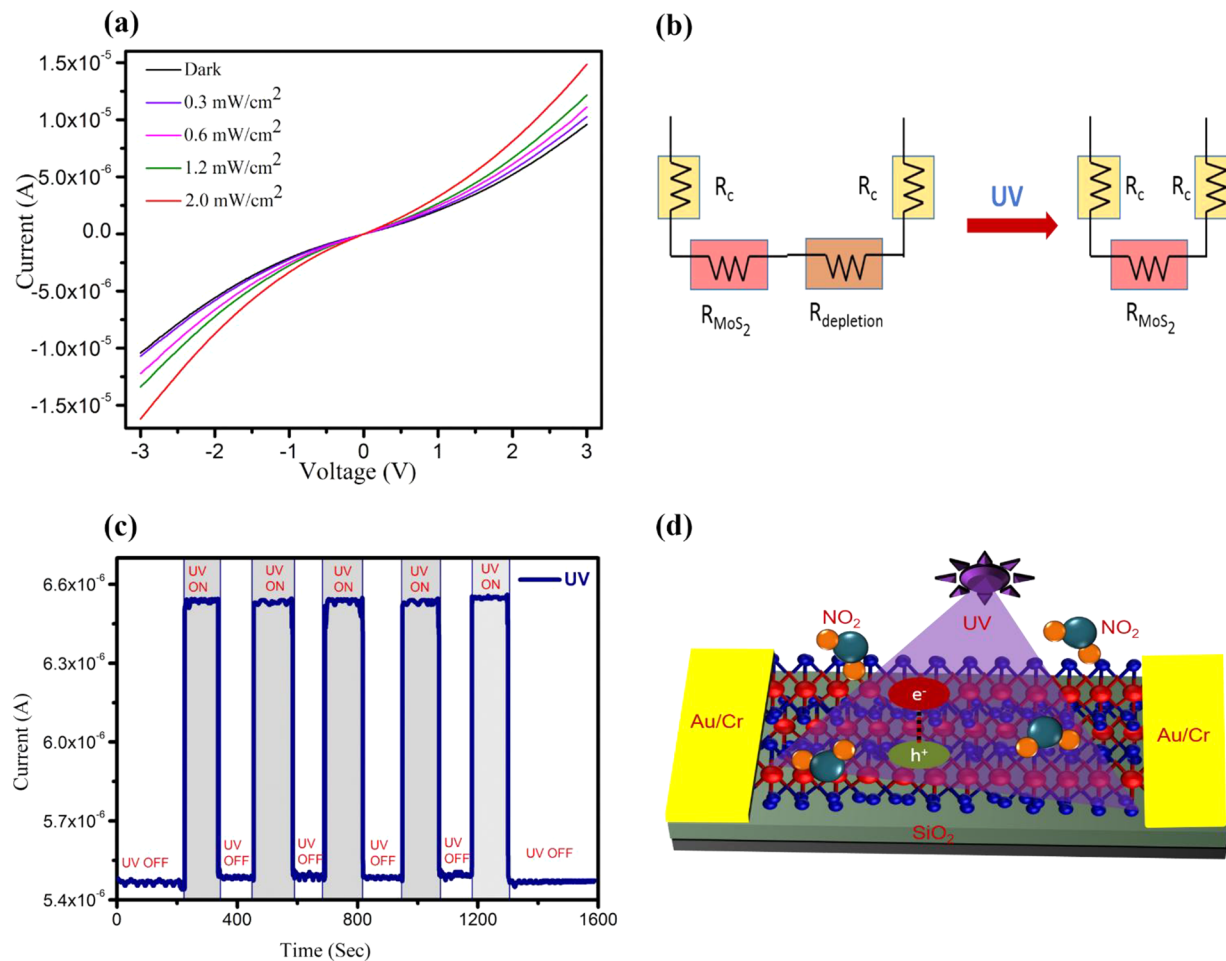


Figure 2. (a) I – V characteristic of the device in the dark and in different intensities of UV light ($0.3, 0.6, 1.2$, and 2 mW/cm^2). (b) Resistance model of the device before/after light. Under photoexcitation, depletion resistance (due to ambient oxygen and humidity) was removed. (c) Current transient characteristics in the presence of UV light at constant voltage. (d) Schematic illustration of chemiresistive sensor in this work.

a rate of $15\text{ }^\circ\text{C}/\text{min}$ up to $550\text{ }^\circ\text{C}$ subsequently at a rate of $25\text{ }^\circ\text{C}/\text{min}$ from 550 to $870\text{ }^\circ\text{C}$. The temperature of sulfur was increased rapidly up to $160\text{ }^\circ\text{C}$ and kept constant throughout the process with Ar flow of 60 sccm at atmospheric pressure.

Characterization and Devices Fabrication. The morphology of as-synthesized MoS₂ on SiO₂/Si was examined by SEM of EVO 18 Zeiss with an accelerating voltage of 20 kV . The Raman spectra of the sample were investigated by Raman spectroscopy (Renishaw single monochromator equipped with a CCD) at room temperature with a laser excitation wavelength of 514 nm . The resistive based gas sensor device was fabricated after depositing two metal electrodes of Au/Cr ($200\text{ nm}/5\text{ nm}$) by thermal evaporation technique using a shadow mask. The distance between two rectangular electrodes and width of the electrode of the device were kept at 100 and $250\text{ }\mu\text{m}$, respectively. After making electrodes, the device was put in a furnace at $200\text{ }^\circ\text{C}$ for 45 min in the N₂ atmosphere to improve contact quality.

Gas Sensing Measurement. Gas sensing behavior of MoS₂ gas sensor was examined in a gas sensing chamber using 5% NO₂ balanced with Ar gas (95% Ar and 5% NO₂). The desired concentration (ppm) of NO₂ was achieved after mixing 5% NO₂ with Ar gas and injecting that concentration into the gas chamber. An external heating filament was used to raise the temperature of the device up to $100\text{ }^\circ\text{C}$. In addition, UV-LED ($\sim 365\text{ nm}$) was used to illuminate the device at room temperature. The intensities of UV light were varied by changing the distance in between sensor and UV source. All the gas sensing measurements were performed under the same conditions in the absence/presence of UV light at room temperature and at $100\text{ }^\circ\text{C}$. Here, the change in current of the device at 2 V bias voltage was measured using Keithley 4200 semiconductor characterization system.

RESULTS AND DISCUSSION

Scanning electron microscopy was carried out to investigate the morphology of as-prepared multilayer MoS₂ film. Figure 1a shows that the micrometer-scaled triangular-shaped MoS₂ flakes are aligned horizontally on SiO₂/Si. The film is uniform everywhere with combined flakes without any 3D structure and wrinkles, which attributes the gas sensing performance to adsorption energy and charge transfer capability of multilayer MoS₂ film only. Standard Raman spectroscopy technique was used to examine the number of layers and crystallinity of the MoS₂ film. Figure 1b indicates the Raman spectra of MoS₂ in which two prominent vibrational mode E_{2g}¹ and A_{1g} are located at $\sim 382\text{ cm}^{-1}$ and $\sim 407\text{ cm}^{-1}$, respectively. The E_{2g}¹ vibrational mode is attributed to in-plane vibration of molybdenum and sulfur atom and the A_{1g} mode is related to out of plane vibration of sulfur atoms.²⁷ The difference between these two vibrational modes was observed as $\sim 25\text{ cm}^{-1}$, indicating multilayer. The difference was the same as reported in previous reports.^{28,29} The full-width half maxima (fwhm) of E_{2g}¹ was determined as ~ 3.82 , which is proof of highly crystalline MoS₂ and approximately consistent with a previous report on CVD grown MoS₂ (3.8).³⁰ Figure 1c,d illustrates the atomic force microscopy (AFM) image and quantitative AFM height profile of MoS₂ flake, respectively, and the measured height of $\sim 3.0\text{ nm}$ indicates a multilayer (4 layer) MoS₂ nanosheet. The

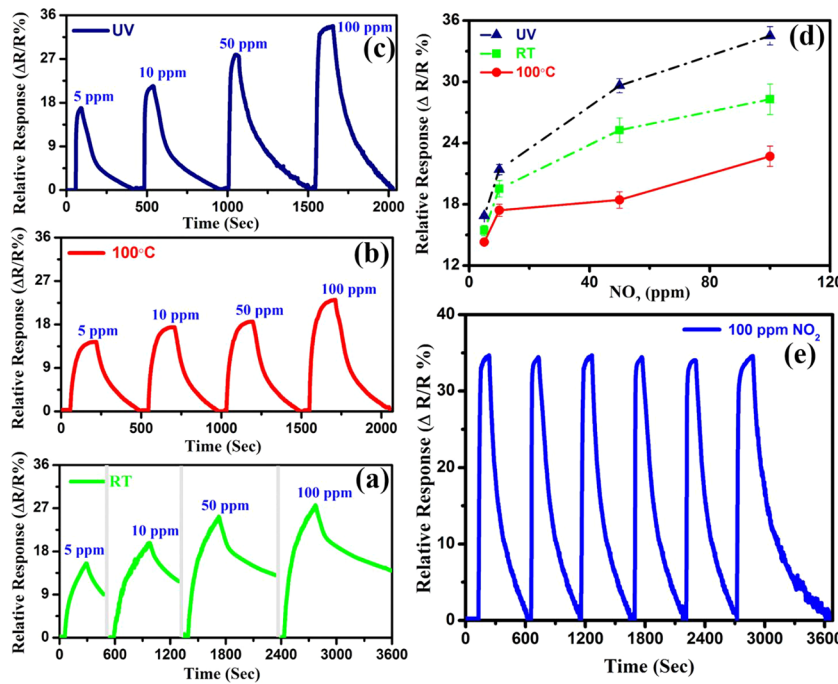


Figure 3. Transient relative response of sensor to 5, 10, 50, and 100 ppm concentration of NO₂ (a) at room temperature (RT), (b) at 100 °C, and (c) at RT under UV-illumination (1.2 mW/cm²). (d) Relative response versus NO₂ concentration at RT, 100 °C, and at RT under light, vertical error bars represent the standard deviation from the mean value. (e) Cyclic test to 100 ppm of NO₂ at RT under UV light.

resistive gas sensor was fabricated with two Au/Cr electrodes on as-synthesized multilayer MoS₂; SEM and optical images are given in Supporting Information Figure S1 a,b, respectively. The current versus voltage (*I*-*V*) characteristic of a multilayer MoS₂ device was investigated in air and vacuum (Figure S2). We observed that current conduction is high in a vacuum as compared to that in air because of p-type doping by ambient oxygen in air. We noticed that nonlinear behavior of *I*-*V* characteristic in a vacuum with Au/Cr electrode indicates the existence of Schottky barrier at the interface. The Schottky barrier height between Au to multilayer MoS₂ was estimated by the following standard thermionic equation

$$I = I_0 \left[\exp\left(\frac{qV}{\eta kT}\right) - 1 \right] \quad (1)$$

where I_0 is the reverse saturation current which can be expressed as

$$I_0 = AA^*T^2 \exp\left(-\frac{q\Phi_B}{kT}\right) \quad (2)$$

in the above eqs, q is the electronic charge, η is the ideality factor, k is the Boltzmann's constant, T is the temperature, A is the contact area, A^* is the effective Richardson's constant (54 A cm⁻² K⁻²), and Φ_B is the Schottky barrier height.

Using eqs 1 and 2, a Schottky barrier height of 0.19 eV is evaluated for this device in a vacuum. Our obtained result is consistent with earlier reports which showed that the Au-MoS₂ contacts cannot be completely ohmic as the binding energy of MoS₂ to Au is very weak.^{46,47} Further, we measured the current of multilayer MoS₂ under the illumination of UV light in a vacuum. Here, the UV intensity was varied as 0.3, 0.6, 1.2, and 2 mW cm⁻², and it was observed that the photocurrent of the device was enhanced with increased UV intensity (Figure 2a). This enhancement in current ascribed to the generation of hot

charge carriers by photoexcitation and cleaning the surface of MoS₂. Figure 2b depicting a schematic of the resistance model of MoS₂ device in the dark and UV light. The reversible switching behavior of current was examined for a multilayer MoS₂ device at constant voltage (2 V) in an inert environment in the presence of UV illumination. From Figure 2c, it is clear that the baseline of current in the MoS₂ gas sensor is stable through the cyclic test. The highly stable device's current after switching on/off the light is proof that the modulation of conductance under photoexcitation is not part of the imperfection of MoS₂. The fast response/recovery of current for multilayer MoS₂ ascribed to fast carrier transport is due to the higher density of state and small energy band gap (1.2 eV). Moreover, optical transition between d orbitals of Mo atoms makes it as a resistant material for photodegradation.

We have investigated systematic gas sensing behavior of MoS₂ toward various concentrations of NO₂ gas in the airtight gas sensing chamber in different environments, and a schematic of the device used in this work is given in Figure 2d. The first, the relative response of MoS₂ gas sensor, was examined under different NO₂ gas concentration range from 5 to 100 ppm at room temperature. The relative response of the sensor was calculated as $(\Delta R/R_o) \times 100\% = (R_g - R_o)/R_o \times 100\%$, where R_g is the resistance of MoS₂ in the gas environment and R_o is the initial resistance of the device in a vacuum. The relative response of multilayer MoS₂ to 5 ppm and increased concentration up to 100 ppm of NO₂ were evaluated ~15.28% and ~27.92% at room temperature, respectively (Figure 3a). It was observed that the relative response of the MoS₂ gas sensor increases with increasing concentration of NO₂ (Figure 3d). This positive relative response of the sensor is attributed to enhancement in resistance of n-type MoS₂ after trapping the electrons by oxidizing NO₂ gas. However, recovery of the device was very poor after degrading the NO₂ (Figure 3a) and unsatisfactory recovery limits the MoS₂ to develop

practical gas sensor at room temperature. Low desorption rate of gas molecules at room temperature of MoS_2 is ascribed to the high binding energy of the NO_2 gas.³¹ Afterward, we have analyzed the sensing performance of MoS_2 at 100 °C using an external resistive heating element and found a relative response of ~12.12% and ~21.56% for 5 and 100 ppm of NO_2 , respectively (Figure 3b). It was noticed that relative response of multilayer MoS_2 device decreases by thermoactivation compared to response at room temperature. However, the baseline of gas sensor was achieved after full desorption of gas molecules (NO_2) from the surface of the sensing layer. The decrement in response under thermal excitation demonstrates that other processes are required to circumvent this issue. To address the challenges related to sensing under thermal energy, we further investigated sensing behavior of the device to NO_2 in the presence of UV light at room temperature. Initially, the sensor was mounted in a sensing chamber under the pressure of $\sim 2 \times 10^{-3}$ mbar and constant baseline was achieved under UV illumination before loading the NO_2 . A UV-LED was switched on during the entire experimental time (loading/delowering of gas in sensing chamber). In order to compare the effect of UV intensities in sensing performance of the multilayer MoS_2 , we investigated the transient relative response of multilayer MoS_2 to 100 ppm of NO_2 under the illumination of different UV intensities ranging from 0.3 to 2 mW/cm². It was noticed that sensitivity of MoS_2 to NO_2 initially increased with increasing intensity up to 1.2 mW/cm² and a sudden decrease in sensitivity was registered when exposed to 2 mW/cm² intensity (Figure S3). The decrement in sensitivity with high intensity is attributed to faster desorption rate than adsorption rate. Moreover, at higher intensity a lower number of excited charge carriers interact with gas molecules. At 1.2 mW/cm² intensity, MoS_2 sensor showed high sensitivity to NO_2 with optimal response and recovery time. So, we investigated the sensing performance of MoS_2 to different concentrations of NO_2 under the 1.2 mW/cm² UV irradiation. The relative response of MoS_2 in the range 5 to 100 ppm of NO_2 were estimated as ~17.82% and ~35.16%, respectively, as shown in Figure 3c. The relative responses of MoS_2 were reached at equilibrium instantly and recover rapidly after loading/delowering the NO_2 in the sensing chamber. Interestingly, the relative response of the sensor was increased with excellent recovery exposure to NO_2 gas at room temperature under optical excitation as compared to response at room temperature and at 100 °C temperature. In order to point out the importance of the reversibility aspect of the practical gas sensor at room temperature, the cyclic test was examined of the multilayer MoS_2 gas sensor to 100 ppm NO_2 at room temperature under UV illumination (1.2 mW/cm²), which is illustrated in Figure 3e. The excellent reversibility of sensor with fast response and minimum recovery time was observed over the repeated test cycles. This reversibility behavior in 2D material based gas sensors at room temperature is not commonly seen due to low desorption rate of the gas. In addition, to verify the role of on/off of UV light in our experiment, we cleaned the surface of MoS_2 using UV light (1.2 mW/cm²) in a vacuum and examined the sensing behavior of cleaned multilayer MoS_2 , while UV light was off during NO_2 loading/delowering from the sensing chamber. We observed that cleaned MoS_2 without photoexcitation could not recover its baseline resistance and also showed the poor sensitivity (see Figure S4).

To gain insight into response time of the sensor, we analyzed transient relative response to 100 ppm of NO_2 in the presence/

absence of UV light at room temperature and at 100 °C, as shown in Figure 4. The response time of the gas sensor was

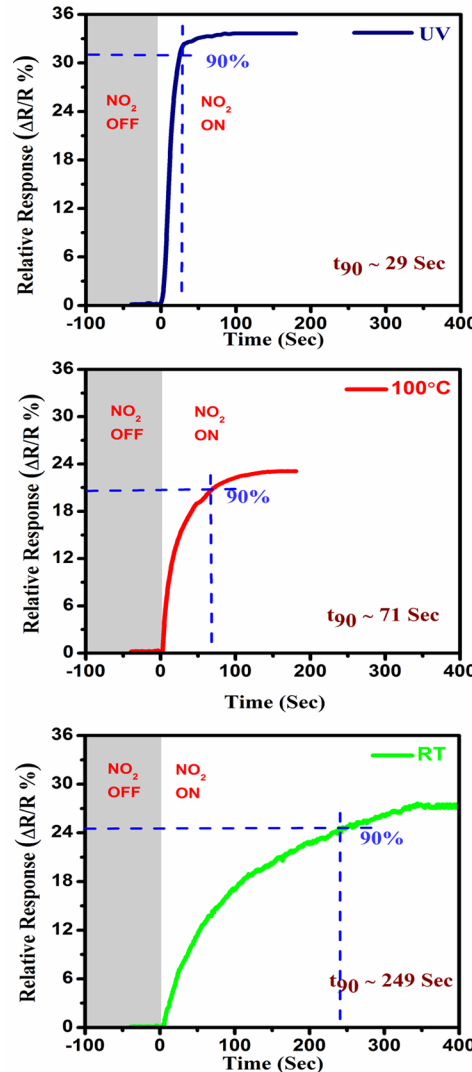


Figure 4. Response time (t_{90}) calculation to 100 ppm of NO_2 at RT, at 100 °C, and at RT under UV (1.2 mW/cm²).

calculated as the time required to achieve 90% of its saturation value in the gas environment. The lowest response time (t_{90}) of ~29 s by optical excitation was achieved as compared to ~71 s using thermoexcitation (100 °C) and ~249 s at room temperature. This ultrafast response time at room temperature is unusually fast compared with previously published reports on MoS_2 gas sensors.^{32,33} Note that the complete recovery of the sensor was also achieved at room temperature under UV illumination, which is also superior to recovery at 100 °C as well as incomplete recovery at room temperature. Furthermore, Figure 5 illustrates the relative response of various gases at different concentrations. To address the selectivity of MoS_2 , the device was exposed to NO_2 , NH_3 , H_2 , H_2S , CO_2 , and CH_4 at room temperature under light illumination. It was found that MoS_2 showed the highest selectivity to NO_2 against the various gases mentioned already.

To date, the exact gas sensing mechanism is elusive, but here it is elucidated based on the degree of charge perturbation on the surface of the sensing layer in the context of NO_2/MoS_2

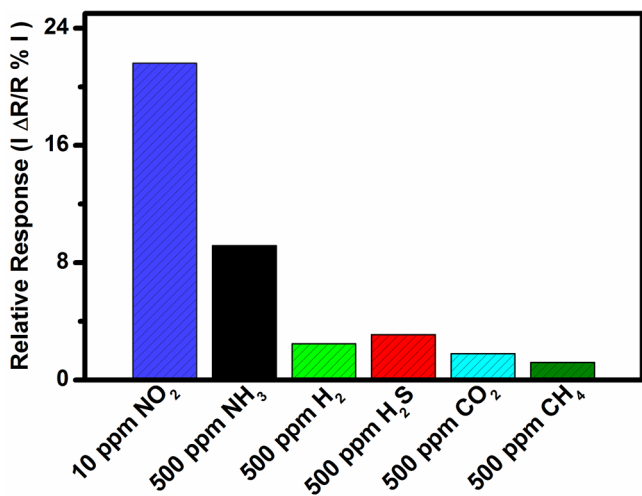


Figure 5. Selectivity histogram of MoS_2 gas sensor at RT under UV illumination. The relative response was measured to 10 ppm of NO_2 and 500 ppm concentration of each of various other gases (NH_3 , CO_2 , H_2 , CH_4 , and H_2S).

interaction, as depicted in Figure 6. The modulation in resistance of MoS_2 directly correlates the concentration and the flow of charge on the surface of MoS_2 before/after adsorption to NO_2 . Sensing behavior is strongly affected by the surface stoichiometry and intrinsic properties of MoS_2 . The ambient oxygen and humidity have been shown the p-type doping effect due to extraction of electrons from MoS_2 .^{34,35} MoS_2 is a typical n-type semiconductor.³⁶ The sensing layer of our sensor is formed by the random connected MoS_2 flakes, and the boundaries of flakes can expose the edge sites, which are highly chemically reactive as compared to the basal plane. Therefore, ambient oxygen, humidity, and contaminants from the CVD fabrication process bonded more with edge sites and also with the defects (anion vacancy) of MoS_2 at room temperature.³⁵ Thereby, absorbed oxygen extracts the electrons

from the MoS_2 and formed O_2^- ion, as shown in following equations.



The electron carrier density of MoS_2 was decreased due to depletion of electrons by ambient oxygen and humidity. In addition, a greater number of reactive sites was occupied by oxygen on the surface of MoS_2 . Upon exposure to NO_2 at room temperature, fewer gas molecules adsorbed on the sensing layer and a lower number of electrons were extracted. On the contrary, thermal energy (temperature $\approx 100^\circ\text{C}$) accelerated the desorption rate compared to the adsorption rate because adsorption energy of NO_2 on MoS_2 is negative (exothermic), which leads to a low response.³⁷ Moreover, higher thermal expansion in the *c*-axis compared to in-plane increased the interlayer distance in layered MoS_2 at high temperature and a surface layer in multilayer MoS_2 behaves like an isolated single layer.^{38–40} So, monolayer MoS_2 showed a low response to NO_2 compared to multilayer MoS_2 . In addition, we hypothesize that the thermal expansion mismatch at the interface of MoS_2 and substrate also showed the minor effect on results because UV-light assisted the reaction on the surface of MoS_2 without heating the substrate.⁴¹ On the other hand, under UV illumination, a photogenerated hole reacted with oxygen ion and formed O_2 (gas); thereby, the surface of MoS_2 was cleaned and had more reactive sites which were unoccupied by contamination and ambient oxygen. Enhanced electrons in the conduction band of n-type MoS_2 were extracted by NO_2 . These phenomena occurred according to the following reaction:

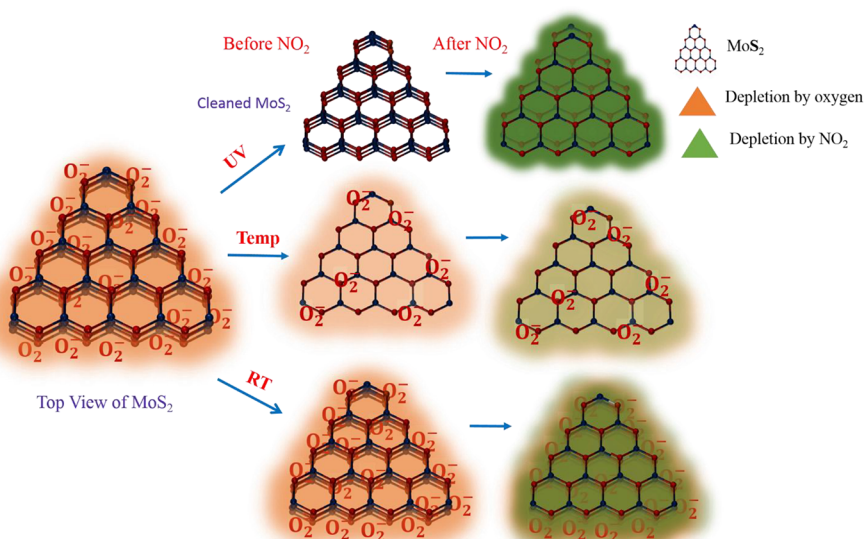
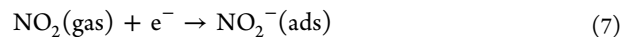
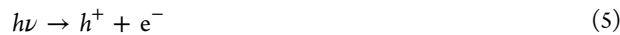


Figure 6. Schematic illustration of the NO_2 gas sensing mechanism with the top view of MoS_2 . Absorbed ambient oxygen at room temperature was removed by temperature. However, it was cleaned perfectly by UV light (UV light was kept on during the experiment). Changes in resistance by NO_2 were highest in the presence of UV light compared to temperature and RT (color intensity shows the number of unoccupied sites on the surface of MoS_2 occupied by NO_2 and depletion region formed).

Table 1. Comparison between Literature on 2D Material Based Gas Sensor and the Present Work (2D MoS₂ Based Gas Sensor)

material	analytes	temperature (°C)	response time	recovery time	references
MoS ₂	100 ppm of NO ₂	RT (UV)	29 s	350 s	This work
MoS ₂	100 ppm of NO ₂	100 °C	71 s	310 s	This work
MoS ₂	100 ppm of NO ₂	RT	249 s	unrecoverable	This work
MoS ₂	20 ppb NO ₂	RT	5–9 min	12 h	16
MoS ₂	100 ppm of NO ₂	RT	3 min	10 min	13
MoS ₂	1.5 ppm of NO	RT	2 min 30 s	3 min unrecoverable	15
p-type MoS ₂	1 ppm of NO ₂	200 °C	11 min	12 min	32
n-type MoS ₂	1 ppm of NO ₂	200 °C	41 min	39 min	32
MoS ₂ /Pd composite	50,000 ppm of H ₂	RT	40 s	83 s	33
MoS ₂ /Graphene	0.5 ppm of NO ₂	200 °C	<1 min	<1 min	19
Graphene nanomesh	10 ppm of NO ₂	RT	5 min	20 min unrecoverable	42
Graphene	5 ppm of NO ₂	RT	5 min	10–12 min	43

As a result, change in the resistance of MoS₂ upon exposure to NO₂ under photoexcitation was higher than under thermoactivation and also at room temperature. After deloading the NO₂ gas, the electrons trapped by the absorbed NO₂ molecules were released back to MoS₂; thereby the baseline was fully recovered by the gas sensor at room temperature. The substantial enhancement in response to full reproducibility of multilayer MoS₂ gas sensor to NO₂ gas at room temperature under the UV illumination was attributed to the removal of contamination from the surface (clean surface, renders greatest possible reactive sites per unit volume) and the minor effect of photogenerated electrons in the conduction band of MoS₂.

Compared to other 2D material based NO₂ gas sensor (see Table 1), our sensor showed fast detection with complete recovery at room temperature under UV illumination. In general, response and recovery time in 2D materials depend on the quick electronic interaction of molecules with the surface of the sensing layer. Photoexcitation is a surface phenomenon, which stimulated the catalytic sensing performance of MoS₂ in terms of the response time through fast surface reaction and established a dynamic equilibrium in between adsorption and desorption processes. On the contrary, thermal excitation increased the temperature of MoS₂ as well as SiO₂ substrate. Heated SiO₂ substrate decreased the mobility of carriers (conduction) of MoS₂ due to resistivity originating from short-range scatterers. The short-range scattering is attributed to intraripple flexural phonons or surface polar phonon in SiO₂.^{44,45} The decreased mobility of MoS₂ under thermal energy was not better at reducing the response time of the sensor as compared to photoexcitation. Moreover, low thermal conductivity of MoS₂ was also responsible for slow response and recovery rate of the sensor. Similarly, MoS₂/graphene hybrid aerogel based sensor showed fast detection and complete recovery to NO₂ because of high electrical and thermal conductivity of graphene.¹⁹

However, using the concept of MoS₂ activation by thermal or optical energy, we cannot explain the sensor's selectivity toward NO₂ against various other gases. The main reason could be greater number of charge (electron) transfer between NO₂ molecules and exposed edge sites on the boundaries of randomly connected MoS₂ flakes, because the theoretical study has shown that NO₂ possesses the highest adsorption energy on the edge sites of MoS₂ as compared to various other gases.^{31,2} Therefore, we can conclude that the demonstrated multilayer MoS₂ based sensor is highly selective to NO₂ at room temperature. This sensing performance of our multilayer

MoS₂ gas sensor at room temperature is profoundly improved from previously reported literature and is listed in Table 1.

CONCLUSION

In summary, we have demonstrated the ultrafast detection and excellent recovery of CVD-grown multilayer MoS₂ to NO₂ at room temperature under UV illumination. We observed the high response time ~249 s and also the incomplete recovery of the MoS₂ sensor at room temperature. After increasing the temperature (100 °C) of the device, full recovery and lower response time ~71 s were achieved at the expense of response. Incomplete recovery at room temperature and poor response at 100 °C were circumvented by photoactivation. The fast recovery, lower response time ~29 s, and high response ~35.16% at room temperature were found for multilayer MoS₂ under UV illumination. Our results reflect an effective approach for the rapid detection with high response, reliable selectivity, and complete recovery to NO₂ by MoS₂ gas sensor at room temperature.

ASSOCIATED CONTENT

Supporting Information

The Supporting Information is available free of charge on the ACS Publications website at DOI: [10.1021/acssensors.7b00731](https://doi.org/10.1021/acssensors.7b00731).

SEM and optical images of device. *I*–*V* characteristic of device in air and vacuum. Transient relative response to NO₂ under different intensities of UV light measurement result. Transient relative response to NO₂ of cleaned MoS₂ surface using UV ([PDF](#))

AUTHOR INFORMATION

Corresponding Author

*E-mail: mkumar@iitj.ac.in.

ORCID

Mahesh Kumar: [0000-0002-5357-7300](https://orcid.org/0000-0002-5357-7300)

Author Contributions

The paper was written through contributions of all authors. All authors have given approval to the final version of the paper.

Notes

The authors declare no competing financial interest.

ACKNOWLEDGMENTS

The authors acknowledge the financial support of the Department of Science and Engineering Research Board-(SERB) Project No. SERB/F/2236/2015-16 dated 16/07/2015.

REFERENCES

- (1) Schwela, D. Air Pollution and Health in Urban Areas. *Rev. Environ. Health* **2000**, *15*, 13–42.
- (2) Cho, S.-Y.; Kim, S. J.; Lee, Y.; Kim, J.-S.; Jung, W.-B.; Yoo, H.-W.; Kim, J.; Jung, H. Highly Enhanced Gas Adsorption Properties in Vertically Aligned MoS₂ Layers. *ACS Nano* **2015**, *9*, 9314–9321.
- (3) Cho, S.-Y.; Lee, Y.; Koh, H.-J.; Jung, H.; Kim, J.-S.; Yoo, H.-W.; Kim, J.; Jung, H.-T. Superior Chemical Sensing Performance of Black Phosphorus: Comparison with MoS₂ and Graphene. *Adv. Mater.* **2016**, *28*, 7020–7028.
- (4) He, Q.; Wu, S.; Yin, Z.; Zhang, H. Graphene-based Electronic Sensors. *Chem. Sci.* **2012**, *3*, 1764–1772.
- (5) Li, H.; Wu, J.; Qi, X.; He, Q.; Liusman, C.; Lu, G.; Zhou, X.; Zhang, H. Graphene Oxide Scrolls on Hydrophobic Substrates Fabricated by Molecular Combing and Their Application in Gas Sensing. *Small* **2013**, *9*, 382–386.
- (6) Xia, F.; Farmer, D. B.; Lin, Y.-M.; Avouris, P. Graphene field effect transistors with high on/off current ratio and large transport band gap at room temperature. *Nano Lett.* **2010**, *10*, 715–718.
- (7) Fang, J.; Wang, D.; DeVault, C. T.; Chung, T. F.; Chen, Y. P.; Boltasseva, A.; Shalaev, V. M.; Kildishev, A. V. Enhanced Graphene Photodetector with Fractal Metasurface. *Nano Lett.* **2017**, *17*, 57–62.
- (8) Robinson, J. T.; Perkins, F. K.; Snow, E. S.; Wei, Z.; Sheehan, P. E. Reduced Graphene Oxide Molecular Sensors. *Nano Lett.* **2008**, *8*, 3137–3140.
- (9) Schedin, F.; Geim, A. K.; Morozov, S. V.; Hill, E. W.; Blake, P.; Katsnelson, M. I.; Novoselov, K. S. Detection of Individual Gas Molecules Adsorbed on Graphene. *Nat. Mater.* **2007**, *6*, 652–655.
- (10) Li, T. S.; Galli, G. L. Electronic Properties of MoS₂ Nanoparticles. *J. Phys. Chem. C* **2007**, *111*, 16192–16196.
- (11) Splendiani, A.; Sun, L.; Zhang, Y. B.; Li, T. S.; Kim, J.; Chim, C. Y.; Galli, G.; Wang, F. Emerging Photoluminescence in Monolayer MoS₂. *Nano Lett.* **2010**, *10*, 1271–1275.
- (12) Natori, K. Ballistic Metal-Oxide-Semiconductor Field Effect Transistor. *J. Appl. Phys.* **1994**, *76*, 4879–4890.
- (13) Late, D. J.; Huang, Y. K.; Liu, B.; Acharya, J.; Shirodkar, S. N.; Luo, J.; Yan, A.; Charles, D.; Waghmare, U. V.; Dravid, V. P.; Rao, C. N. R. Sensing Behavior of Atomically Thin-Layered MoS₂ Transistors. *ACS Nano* **2013**, *7*, 4879–4891.
- (14) Guarneri, M.; Balmes, J. R. Outdoor Air Pollution and Asthma. *Lancet* **2014**, *383*, 1581–1592.
- (15) Li, H.; Yin, Z.; He, Q.; Li, H.; Huang, X.; Lu, G.; Fam, D. W. H.; Tok, A. I. Y.; Zhang, Q.; Zhang, H. Fabrication of Single layer and Multilayer MoS₂ Film-Based Field-Effect Transistors for Sensing NO at Room Temperature. *Small* **2012**, *8*, 63–67.
- (16) Liu, B.; Chen, L.; Liu, G.; Abbas, A. N.; Fathi, M.; Zhou, C. High-Performance Chemical Sensing Using Schottky-Contacted Chemical Vapor Deposition Grown Monolayer MoS₂ Transistors. *ACS Nano* **2014**, *8*, 5304–5314.
- (17) Cho, B.; Kim, A. R.; Park, Y.; Yoon, J.; Lee, Y. J.; Lee, S.; Yoo, T. J.; Kang, C. G.; Lee, B. H.; Ko, H. C.; Kim, D.-H.; Hahm, M. G. Bifunctional Sensing Characteristics of Chemical Vapor Deposition Synthesized Atomic-Layered MoS₂. *ACS Appl. Mater. Interfaces* **2015**, *7*, 2952–2959.
- (18) Fowler, J. D.; Allen, M. J.; Tung, V. T.; Yang, Y.; Kaner, R. B.; Weiller, B. H. Practical Chemical Sensors from Chemically Derived Graphene. *ACS Nano* **2009**, *3*, 301–306.
- (19) Long, H.; Trochimczyk, A. H.; Pham, T.; Tang, Z.; Shi, T.; Zettl, A.; Carraro, C.; Worsley, M. A.; Maboudian, R. High Surface Area MoS₂/Graphene Hybrid Aerogel for Ultrasensitive NO₂ Detection. *Adv. Funct. Mater.* **2016**, *26*, 5158–5165.
- (20) Choi, H.; Choi, J. S.; Kim, J.-S.; Choe, J.-H.; Chung, K. H.; Shin, J.-W.; Kim, J. T.; Youn, D.-H.; Kim, K.-C.; Lee, J.-I.; et al. Flexible and Transparent Gas Molecule Sensor Integrated with Sensing and Heating Graphene Layers. *Small* **2014**, *10*, 3685–3691.
- (21) Park, S.; An, S.; Mun, Y.; Lee, C. UV-Enhanced NO₂ Gas Sensing Properties of SnO₂-Core/ZnO-Shell Nanowires at Room Temperature. *ACS Appl. Mater. Interfaces* **2013**, *5*, 4285–4292.
- (22) Fan, S. W.; Srivastava, A. K.; Dravid, V. P. UV-activated room-temperature gas sensing mechanism of polycrystalline ZnO. *Appl. Phys. Lett.* **2009**, *95*, 142106–3.
- (23) Jaisutti, R.; Lee, M.; Kim, J.; Choi, S.; Ha, T.-J.; Kim, J.; Kim, H.; Park, S. K.; Kim, Y.-H. Ultrasensitive Room-Temperature Operable Gas Sensors Using p-Type Na: ZnO Nanoflowers for Diabetes Detection. *ACS Appl. Mater. Interfaces* **2017**, *9*, 8796–8804.
- (24) Mitoma, N.; Nouchi, R.; Tanigaki, K. Enhanced sensing response of oxidized graphene formed by UV irradiation in water. *Nanotechnology* **2015**, *26*, 105701.
- (25) Chen, G.; Paronyan, T. M.; Pigos, E. M.; Harutyunyan, A. R. Enhanced gas sensing in pristine carbon nanotubes under continuous ultraviolet light illumination. *Sci. Rep.* **2012**, *2*, 343.
- (26) Khan, M. F.; Iqbal, M. W.; Iqbal, M. Z.; Shehzad, M. A.; Seo, Y.; Eom, J. Photocurrent Response of MoS₂ Field-Effect Transistor by Deep Ultraviolet Light in Atmospheric and N₂ Gas Environments. *ACS Appl. Mater. Interfaces* **2014**, *6*, 21645–21651.
- (27) Verble, J. L.; Wieting, T. J. Lattice Mode Degeneracy in MoS₂ and Other Layer Compounds. *Phys. Rev. Lett.* **1970**, *25* (6), 362–365.
- (28) Lee, Y. H.; Zhang, X. Q.; Zhang, W. J.; Chang, M. T.; Lin, C. T.; Chang, K. D.; Yu, Y. C.; Wang, J. T. W.; Chang, C. S.; Li, L. J.; et al. Synthesis of Large-Area MoS₂ Atomic Layers with Chemical Vapor Deposition. *Adv. Mater.* **2012**, *24*, 2320–2325.
- (29) Liu, K. K.; Zhang, W. J.; Lee, Y. H.; Lin, Y. C.; Chang, M. T.; Su, C.; Chang, C. S.; Li, H.; Shi, Y. M.; Zhang, H.; et al. Growth of Large-Area and Highly Crystalline MoS₂ Thin Layers on Insulating Substrates. *Nano Lett.* **2012**, *12*, 1538–1544.
- (30) Wang, S.; Rong, Y.; Fan, Y.; Pacios, M.; Bhaskaran, H.; He, K.; Warner, J. H. Shape Evolution of Monolayer MoS₂ Crystals Grown by Chemical Vapor Deposition. *Chem. Mater.* **2014**, *26*, 6371–6379.
- (31) Yue, Q.; Shao, Z.; Chang, S.; Li, J. Adsorption of gas molecules on monolayer MoS₂ and effect of applied electric field. *Nanoscale Res. Lett.* **2013**, *8*, 425.
- (32) Donarelli, M.; Prezioso, S.; Perrozzi, F.; Bisti, F.; Nardone, M.; Giancaterini, L.; Cantalini, C.; Ottaviano, L. Response to NO₂ and other gases of resistive chemically exfoliated MoS₂-based gas sensors. *Sens. Actuators, B* **2015**, *207*, 602–613.
- (33) Kuru, C.; Choi, C.; Kargar, A.; Choi, D.; Kim, Y. J.; Liu, C. H.; Yavuz, S.; Jin, S. MoS₂ Nanosheet-Pd Nanoparticle Composite for Highly Sensitive Room Temperature Detection of Hydrogen. *Adv. Sci.* **2015**, *2*, 1500004.
- (34) Qiu, H.; Pan, L.; Yao, Z.; Li, J.; Shi, Y.; Wang, X. Electrical characterization of back-gated bi-layer MoS₂ field-effect transistors and the effect of ambient on their performances. *Appl. Phys. Lett.* **2012**, *100*, 123104–3.
- (35) Baker, R. T. K.; Chludzinski, J. J., Jr.; Sherwood, R. D. In-situ electron microscopy study of the reactivity of molybdenum disulphide in various gaseous environments. *J. Mater. Sci.* **1987**, *22*, 3831–3842.
- (36) Zhang, Y.; Ye, J.; Matsuhashi, Y.; Iwasa, Y. Ambipolar MoS₂ Thin Flake Transistors. *Nano Lett.* **2012**, *12*, 1136–1140.
- (37) Cho, B.; Hahm, M. G.; Choi, M.; Yoon, J.; Kim, A. R.; Lee, Y. J.; Park, S. J.; Kwon, J.; Kim, C. S.; Song, M.; Jeong, Y.; Nam, K.; Lee, S.; Yoo, T. J.; Kang, C. G.; Lee, B. H.; Ko, H. C.; Ajayan, P. M.; Kim, D.-H. Charge-transfer-based Gas Sensing Using Atomic-layer MoS₂. *Sci. Rep.* **2015**, *5*, 8052.
- (38) Murray, R.; Evans, B. L. The Thermal Expansion of 2H-MoS₂ and 2H-WSe₂ between 10 and 320 K. *J. Appl. Crystallogr.* **1979**, *12*, 312–315.
- (39) El-Mahalawy, S. H.; Evans, B. L. The Thermal Expansion of 2H MoS₂, 2H-MoSe₂ and 2H-WSe₂ between 20 and 800 °C. *J. Appl. Crystallogr.* **1976**, *9*, 403–406.
- (40) Sahoo, S.; Gaur, A. P. S.; Ahmadi, M.; Guinel, M. J. F.; Katiyar, R. S. Temperature-Dependent Raman Studies and Thermal Con-

ductivity of Few-Layer MoS₂. *J. Phys. Chem. C* **2013**, *117* (17), 9042–9047.

(41) Prades, J. D.; Diaz, R.-J.; Ramirez, F. H.; Barth, S.; Cirera, A.; Rodriguez, A. R.; Mathur, S.; Morante, J. R. Equivalence between thermal and room temperature UV light-modulated responses of gas sensors based on individual SnO₂ nanowires. *Sens. Actuators, B* **2009**, *140*, 337–341.

(42) Paul, R. K.; Badhulika, S.; Saucedo, N. M.; Mulchandani, A. Graphene Nano mesh as Highly Sensitive Chemiresistor Gas Sensor. *Anal. Chem.* **2012**, *84*, 8171–8178.

(43) Randeniya, L. K.; Shi, H. Q.; Barnard, A. S.; Fang, J. H.; Martin, P. J.; Ostrikov, K. Harnessing the Influence of Reactive Edges and Defects of Graphene Substrates for Achieving Complete Cycle of Room-Temperature Molecular Sensing. *Small* **2013**, *9*, 3993–3999.

(44) Chen, J. H.; Jang, C.; Ishiqami, M.; Fuhrer, M. S. Intrinsic and extrinsic performance limits of graphene devices on SiO₂. *Nat. Nanotechnol.* **2008**, *3*, 206–209.

(45) Brivio, J.; Alexander, T. L. D.; Kis, A. Ripples and Layers in Ultrathin MoS₂ Membranes. *Nano Lett.* **2011**, *11*, 5148–5153.

(46) Popov, I.; Seifert, G.; Tomanek, D. Designing Electrical Contacts to MoS₂ Monolayers: A Computational Study. *Phys. Rev. Lett.* **2012**, *108*, 156802–5.

(47) Ganatra, R.; Zhang, Q. Few-Layer MoS₂: A Promising Layered Semiconductor. *ACS Nano* **2014**, *8*, 4074–4099.